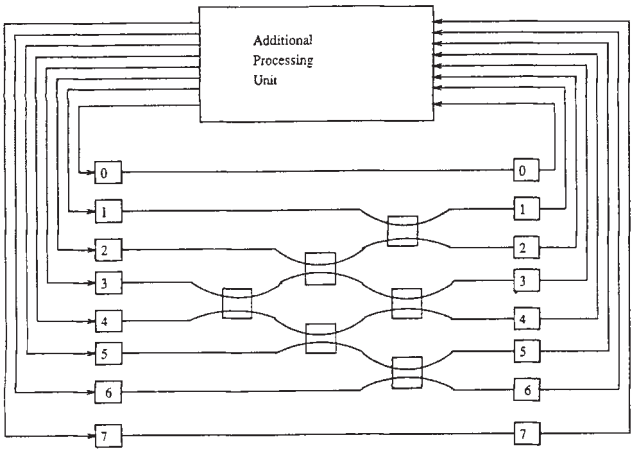

Figure 7 Optical implementation to perform an eight-point FFT using PS

PS has the shape of a binary tree, with the exception that each element in this tree accepts two inputs and yields two outputs, while in a binary tree each element except the root accepts one input and generates two outputs.

Consider the application of the PS in realizing an FFT operation. The butterfly diagram of an eight-point FFT based on the decimation-in-frequency algorithm [13] is shown in Figure 6, where

$$X[k] = \sum_{n=0}^{N-1} x[n]W_N^{kn}; \qquad k = 0, 1, 2, \ldots, N-1 \quad (10)$$

and

$$W_N^{kn} = e^{-j2\pi kn/N}; \qquad n = 0, 1, 2, \ldots, N-1. \quad (11)$$

We observe that the interconnections involved change at different stages of the FFT [6, 13]. Therefore, instead of changing the interconnection at each stage, a fixed PS network can be applied repeatedly to achieve the desired inerconneciton pattern. An optical setup for repeated application of the PS to perform FFT is shown in Figure 7, where the input signals, after passing through the PS network, are fed back to the corresponding locations of the input waveguides or optical fibers and the PS operation is repeated on the feeback pattern. The feedback path may also be realized using a combination of beam splitter and mirrors. Note that adiditonal processing on the output signals is necessary (to adjust the W_N^{kn} coefficients) before repeating the PS operation. This process is repeated at each stage of Figure 6 until the desired pattern is obtained at the output. For an N-point FFT, for example, the PS operation should be repeated $\log_2 N$ times. The system shown in Figure 7 may also be used to implement other parallel processing algorithms like Batcher's bitonic sort algorithm.

5. CONCLUSION

An efficient implementation of the PS interconnection network using Fredkin gates has been presented. When compared to the other existing networks, this implementation is programmable and cost effective. Desired patterns can be generated at the output of the PS by appropriately programming the control signal. Larger size PS networks can be constructed by connecting a smaller size fixed PS network in a treelike structure. Optical implementation to perform PS repeatedly is shown, which is useful to implement various parallel processing algorithms. The PS implementation can also be used for arbitration schemes in multiprocessor systems. The information transfer rate through the network can be doubled if two signals with different polarization modes (such as horizontal and vertical) were to be transmitted through the same channel.

REFERENCES

1. A. W. Lohmann, "What Classical Optics Can Do for the Digital Optical Computer," *Appl. Opt.*, Vol. 25, 1986, pp. 1543–1549.
2. A. W. Lohmann, W. Stork, and G. Stucke, "Optical Perfect Shuffle," *Appl. Opt.*, Vol. 25, 1986, pp. 1530–1531.
3. K. H. Brenner and A. Huang, "Optical Implementations of the Perfect Shuffle Interconnection," *Appl. Opt.*, Vol. 27, 1988, pp. 135–1137.
4. A. A. Sawchuk, B. K. Jenkins, C. S. Raghavendra, and A. Varma, "Optical Crossbar Networks," *Computer*, Vol. 20, 1987, pp. 50–60.
5. J. Shamir and J. H. Caulfield, "High Efficiency Rapidly Programmable Optical Interconnections," *Appl. Opt.*, Vol. 26, 1987, pp. 1032-1037.
6. H. S. Stone, "Parallel Processing with the Perfect Shuffle," *IEEE Trans. Comput.*, Vol. C-20, 1971, p. 153.
7. C. L. Wu and T. Y. Feng, "The Universality of Shuffle-Exchange Network," *IEEE Trans. Comput.*, Vol. C-30, 1981, p. 324.
8. E. Fredkin and T. Toffoli, "Conservative Logic," *Int. J. Theor. Phys.*, Vol. 21, 1982, pp. 219–253.
9. R. Cuykendall and D. McMillan, "Control-Specific Fredkin Circuits," *Appl Opt.*, Vol. 26, 1987, pp. 1959–1963.
10. J. Shamir, J. H. Caulfield, W. Micelli, and R. J. Seymour, "Optical Computing Using Fredkin Gates," *Appl Opt.*, Vol. 25, 1986, pp. 1604–1607.
11. J. W. Goodman, F. J. Leonberger, S. Y. Kung, and R. A. Athale, "Optical Interconnections for VLSI Systems," *Proc. IEEE*, Vol. 72, 1984, pp. 850–866.
12. B. D. Clymer and J. W. Goodman, "Optical Clock Distribution to Silicon Chips," *Opt. Eng.*, Vol. 25, 1986, pp. 1103–1108.
13. A. V. Oppenheim and R. W. Schafer, *Discrete-Time Signal Processing*, Prentice Hall, Englewood Cliffs, NJ, 1989.

Received 1-16-92

Microwave and Optical Technology Letters, 5/7, 330–333

CCC 0895-2477/92/$4.00

H-SCATTERING OF THIN-FILM MODES FROM PERIODIC GRATINGS OF FINITE EXTENT

Andrey S. Andrenko and Alexander I. Nosich
Institute of Radiophysics and Electronics
Ukrainian Academy of Sciences
Kharkov 310085, Ukraine

KEY TERMS

Dielectric waveguide, inhomogeneity, grating coupler, scattering pattern

ABSTRACT

Dielectric thin-film guided mode scattering from a finite-element periodic grating of circular wires or circularly curved metal strips is considered. An accurate solution method is developed and results of computations for the H case are given. © *1992 John Wiley & Sons, Inc.*

INTRODUCTION

Dielectric-film waveguides with periodic inhomogeneities are of considerable interest in connection with distributed-feedback and distributed-Bragg-reflection lasers, integrated optical filters, grating couplers, millimeter-wave antennas, etc. The vast amount of works in grating coupler theories and their applications can be found for dielectric waveguides with periodically grooved or corrugated surface structures of finite and infinite extent [1–5].

All these theories are approximate; however, there exist certain canonical geometries for which exact numerical solutions are obtainable. In this article we present an accurate method of solution for thin-film guided H-polarized mode scattering from a finite number of metal objects shaped as circular closed or open cylinders. The method follows the previously reported work [6, 7] on the scattering by a single screen in dielectric-slab waveguide. Althoug this approach is equally valid for arbitrarily positioned scatterers, the periodically arranged collection of elements is investigated, and some numerical results about far-field scattering patterns are presented.

FORMULATION OF THE PROBLEM

The geometry of the analyzed problem is illustrated in Figure 1. Thin-film waveguide consists of a dielectric medium of thickness $2d$ and permittivity ϵ sandwiched between two free half spaces. Time dependence is assumed in the form $\exp(-i\omega t)$ and is suppressed everywhere. Thin film is known to support a finite number of modes (surface waves) of two types: TE_j, having only z component of electric field, and TM_j, having only z component of magnetic field ($j = 0, 1, \ldots, Q^{e,m}$, $Q^{e,m}$ are the numbers of modes). Note that the TE/TM designation of these modes is based on the field structure with respect to the direction of propagation.

Let one of the modes be incident on a finite-periodic grating of N cylindrical obstacles places inside the film normal to the direction of mode propagation. It is obvious that for TE_j incident mode we have an E-polarized scattering problem with respect to the cylinders' axis, while for TM_j mode case we have an H-polarized scattering problem. Our article deals with the H-polarized case although the general approach is equally suitable for alternative polarization.

We consider the structure with elements of the shape of either closed or zero-thickness nonclosed circular cylinders with perfect conductivity.

Assume the scalar function $H(\mathbf{r})$ to correspond to the H_z component of the total electromagnetic field and decompose it to incident field and scattered field terms like

$$H(\mathbf{r}) = H^0(\mathbf{r}) + H^{sc}(\mathbf{r}) = H^0(\mathbf{r}) + \sum_{s=1}^{N} H_s^{sc}(\mathbf{r}), \quad (1)$$

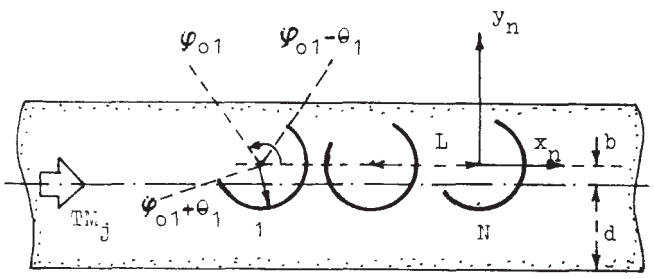

Figure 1 Scattering problem geometry for a thin-film waveguide

where $H_s^{sc}(\mathbf{r})$ is the field generated by currents induced on the sth scatterer.

The incident field is that of one of the guided modes, so

$$H^0(\mathbf{r}) = V_j^{e,0}(y)\exp(ih_j x) = \begin{cases} v^{e,0}(p_j y), & |y| \le d \\ v^{e,0}(p_j d)\exp[ig_j(|y| - d)], & |y| \ge d \end{cases} \exp(ih_j x), \quad (2)$$

where $g_j = (k^2 - h_j^2)^{1/2}$, $p_j = (k^2\epsilon - h_j^2)^{1/2}$, $v^e(\cdot) = \cos(\cdot)$, $v^0(\cdot) = \sin(\cdot)$

The functions H^0 and H^{sc} have to satisfy the 2D Helmholtz equation

$$[\Delta + k^2\epsilon(\mathbf{r})]H(\mathbf{r}) = 0, \quad \mathbf{r} \in R^2\backslash\{y = \pm d, M_s, s = 1, \ldots, N\} \quad (3)$$

with the piece-constant coefficient $\epsilon(r) = \epsilon$ for $|y| \le d$ and elsewhere, continuity conditions on the slab's interfaces

$$[H] = 0, \qquad [\epsilon^{-1}\partial H/\partial y] = 0, \qquad y = \pm d, \quad (4)$$

where square brackets are for the jumps of functions, and Neumann boundary conditions on the scatterers

$$\partial H(\mathbf{r})/\partial n_s = 0, \qquad \mathbf{r} \in M_s, \qquad s = 1, \ldots, N \quad (5)$$

completed with the Meixner-type edge condition in the event of nonclosed contours of M_s, namely,

$$\int_D (k^2\epsilon\,|H|^2 + |\text{grad } H|^2)\,d\mathbf{r} < \infty \quad (6)$$

for any bounded domain D containing edges, and, finally, a condition of radiation at infinity modified in comparison with the well-known Sommerfeld one. Mathematically correct treatment yields the asymptotic expression which takes into account the discrete spectrum of film's natural guided modes as well as the part of the field propagating in the form of cylindrical wave:

$$H^{sc}(\mathbf{r}) \underset{r\to\infty}{\sim} \begin{cases} \Phi_j^{(\pm)}(\phi)\left(\dfrac{2}{i\pi kr}\right)^{1/2} e^{ikr}, & y \ge \pm d \\ 0, & |y| < d \end{cases} + \sum_{q=1}^{Q} \begin{cases} T_{qj} - \delta_{qj}, & x > 0 \\ R_{qj}, & x < 0 \end{cases} V_q(y)\exp(ih_q|x|). \quad (7)$$

The far-field scattering patterns $\Phi_j^{(\pm)}(\phi)$ and mode conversion coefficients T_{qj}, R_{qj} are the quantities to be found.

ANALYTICAL-NUMERICAL SOLUTION

The scattered field is sought as a sum of N generalized double-layer potentials

$$H_s^{sc}(\mathbf{r}) = \int_{M_s} \mu^s(\mathbf{r}_s)\frac{\partial}{\partial n_s} G(\mathbf{r}, \mathbf{r}_s)\,d\mathbf{r}_s, \qquad s = 1, N, \quad (8)$$

where $\mathbf{r}_s \in M_s$, $\mu^s(\mathbf{r})$ is the induced surface current density function, and $G(\mathbf{r}, \mathbf{r}_s)$ is the Green's function of the film, which can be presented as a Fourier-type integral of known

functions inside and outside the film. For example, if $|y|$, $|y_s| < d$, then

$$G(\mathbf{r}, \mathbf{r}_s) = \frac{i}{4} H_0^{(1)}(k\epsilon^{1/2} |\mathbf{r} - \mathbf{r}_s|) + \frac{i}{4\pi} \int_C F(y, y_s, h) e^{ih(x-x_s)}\, dh, \quad (9)$$

where

$$F(y, y_s, h) = \left(1 - \frac{\epsilon g}{p}\right) e^{ipd} \left[i \frac{\cos(py)\cos(py_s)}{\Delta_1(h)} + \frac{\sin(py)\sin(py_s)}{\Delta_2(h)} \right], \quad (10)$$

with $g = (k^2 - h^2)^{1/2}$, $p = (k^2\epsilon - h^2)^{1/2}$, and

$$\Delta_1(h) = ig\epsilon \cos(pd) + p \sin(pd), \quad (11)$$

$$\Delta_2(h) = ig\epsilon \sin(pd) - p \cos(pd). \quad (12)$$

The equations $\Delta_1(h) = 0$ and $\Delta_2(h) = 0$ are the dispersive equations determining natural modes of the film. Purely real roots of them are for guided surface modes of even (TM_{2n}) and odd (TM_{2n+1}, $n = 0, 1, \ldots$) types, respectively, while complex roots are for leaky waves and other complex waves. For any fixed set of values of kd and ϵ, there exists a finite number of surface TM modes of both types, the lowest of them, TM_0, having no low-frequency cutoff.

To find the unknown current densities $\mu^s(\mathbf{r})$, one must subject the field (1), (8) to the boundary conditions (5) and seek the solution ensuring convergence of (6). This leads to the set of N singular integrodifferential equations valid on the contours M_s, $s = 1, \ldots, N$.

Then functions $\mu^s(\mathbf{r})$ are expanded in terms of an angular Fourier series in a local coordinate of corresponding scatterer

$$\mu^s(\phi_s) = (2/i\pi k\epsilon^{1/2}a) \sum_{(n)} \mu_n^s e^{in\phi_s}, \qquad s = 1, \ldots, N, \quad (13)$$

with unknown coefficients μ_n^s ($n = 0, \pm 1, \ldots$), and similar expansions are derived for the Green's function and the incident field. Substituting all these expansions to integrodifferential equations enables one to make term-by-term operations and come to N systems of dual series equations;

$$\sum_{(n)} \left\{ \mu_n^s \left(J_n' H_n' e^{in\phi_s} + J_{-n}' \sum_{(m)} J_m' \Omega_{nm} e^{im\phi_s} \right) + f_n^s e^{in\phi_s} + \sum_{q=1, \neq s}^{N} \mu_n^q \left[J_n' \sum_{(m)} H_{n-m}^{(1)}(k\epsilon^{1/2}L\,|q-s|) J_m' e^{i(n-m)\phi_{qs}} e^{im\phi_s} + J_{-n}' \sum_{(t)} \Omega_{nt} \sum_{(m)} J_{t-m}(k\epsilon^{1/2}L\,|q-s|) J_m' e^{i(t-m)\phi_{qs}} e^{im\phi_s} \right] \right\} = 0$$

$$\theta_s < |\phi_s - \phi_{0s}| \le \pi,$$

$$\sum_{(n)} \mu_n^s e^{in\phi_s} = 0, \qquad |\phi_s - \phi_{0s}| < \theta_s, \qquad s = 1, \ldots, N, \quad (14)$$

where $J_n' = J_n'(k\epsilon^{1/2}a)$, $H_n' = H_n'(k\epsilon^{1/2}a)$, $\phi_{qs} = 0$, if $q < s$ or π if $q > s$,

$$\Omega_{nt} = \frac{i^{n+t+1}}{\pi} \int \left(1 - \frac{\epsilon g}{p}\right) e^{ipd} \left[\frac{\cos(n\psi + pb)\cos(t\psi + pb)}{\Delta_1(h)} - i \frac{\sin(n\psi + pb)\sin(t\psi + pb)}{\Delta_2(h)} \right] dh, \quad (15)$$

$$f_n^s = i^n J_n' v^{e,0}(n\psi_j + p_j b) \exp[ih_j L(s-1)], \quad (16)$$

and $\psi^{(j)}$ is defined by means of expressions

$$\cos \psi_{(j)} = h_{(j)}/k\epsilon^{1/2}, \qquad \sin \psi_{(j)} = -p_{(j)}/k\epsilon^{1/2}. \quad (17)$$

Besides, the edge condition is reduced to a set of inequalities

$$\sum_{(n)} |\mu_n^s|^2 |n+1| < \infty, \qquad s = 1, \ldots, N. \quad (18)$$

Dual series equations like (14) can be effectively regularized by means of the partial inversion procedure based on the Riemann-Hilbert problem technique. The term inverted analytically corresponds to small-argument approximation of the product of cylindrical functions derivatives in (14), i.e., to the static part of the dual series operator. Resulting equations for the unknown coefficients can be written, in the matrix-operator form, as

$$\left[I + \sum_{t=1}^{N} (A_1^{st} + A_2^{st}) \mu^t \right] = B^s, \qquad s = 1, \ldots, N, \quad (19)$$

where the operator I is the identity operator, and operators $A_{1,2}^{st}$ are compact in some functional space provided that the screens do not intersect each other and the surfaces of the slab. Note that operators A_1^{ss}, $A_1^{ss} + A_2^{ss}$ are the same as for the free space and slab mode scattering by a single sth screen, respectively, while operators $A_{1,2}^{st}$ describe the interaction between the sth and tth elements of the obstacle. Compactness of the mentioned operators ensures the convergence of approximate solutions obtained through truncation to exact ones with increasing matrix order.

As for the far-field parameters, they can be calculated with the aid of a series:

$$\begin{pmatrix} T_{mj} - \delta_{mj} \\ R_{mj} \end{pmatrix} = \frac{2(\epsilon g_m - p_m) e^{ip_m d}}{p_m \Delta_{1,2}'(h)} \times \sum_{(n)} (\pm i)^n J_n' v^{e,0}(p_m b \pm n\psi_m) M_n(\pm h_m), \quad (20)$$

$$\Phi_j^{(\pm)}(\phi) = \frac{k \sin\phi e^{ip'd}}{p} \times \sum_{(n)} \left\{ (-i)^n J_n' \left[(\epsilon g' - p') \left(\frac{\cos p'd \cos(n\psi' + p'b)}{i\Delta_1(k\cos\phi)} \mp \Delta_2^{-1}(k\cos\phi) \sin p'd \sin(n\psi' + p'b) \right) + e^{\mp ip'b - in\psi'} \right] \right\} M_n(k\cos\phi), \quad (21)$$

where $g' = g(k \cos \phi)$, $p' = p(k \cos \phi)$, $\phi = (0, \pi)$, and the functions

$$M_n(h) = \sum_{s=1}^{N} \mu_n^s e^{ihL(s-1)}, \qquad n = 0, \pm 1, \ldots \tag{22}$$

serve for angular coefficients of equivalent current density induced on some effective circular scatterer (made of N ones) as it is seen from infinity inside or outside the film.

NUMERICAL RESULTS AND DISCUSSION

Computations of the scattering characteristics have been made by employing numerical procedures to the equations obtained above and truncated to the order N_{tr} = entire part of $(k\epsilon^{1/2}a) + 5$ to ensure the accuracy of 0.1%.

Although the formal solution given by (19) is valid for any type of the incident field, the case of a single-mode propagation is obviously the most interesting for applications. To cut all the higher modes off, one must operate with a dielectric film satisfying the condition $kd(\epsilon - 1)^{1/2} < \pi/2$.

So, all the results given in this section are for the film with parameters $kd = 1$, $\epsilon = 2.25$ that provides the wave number of the incident principal mode TM_0 to be $h_0/k = 1.16$.

In Figure 2, the far-field scattering patterns are presented for the grating scatterer of circular perfectly conducting wires with the radius $a = 0.07d$. Figure 2(a) corresponds to $N = 7$ elements with grating parameter $\kappa = L/\lambda = 0.117$, i.e., for a short periodic one. The radiation due to the scattering can be seen to occur mainly to the backward half space, similarly to the free-space scattering by a small body. The effect of the film is in nulling the far-field amplitudes in the grazing direction $\phi = 0, \pi$. Thus, along the film the power is carried solely by the guided modes.

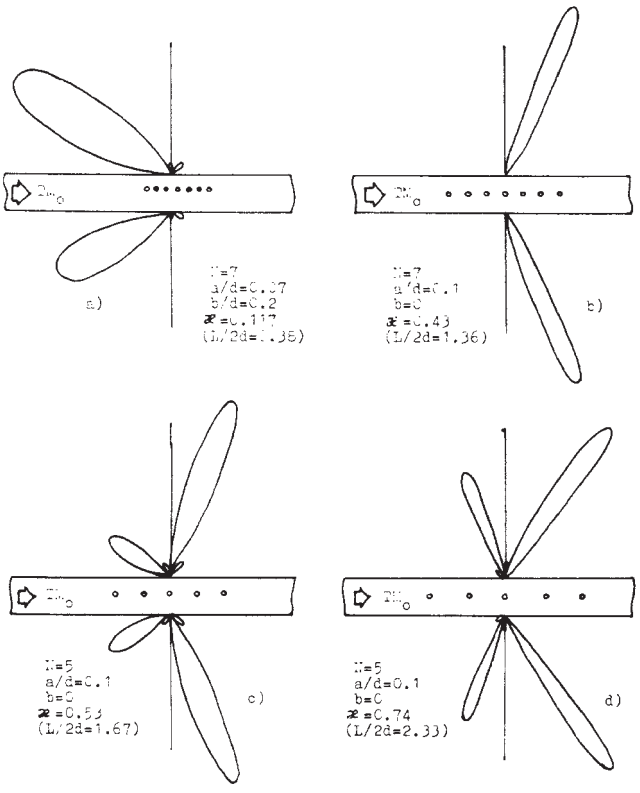

Figure 2 Normalized far-field scattering patterns for a grating of circular wires

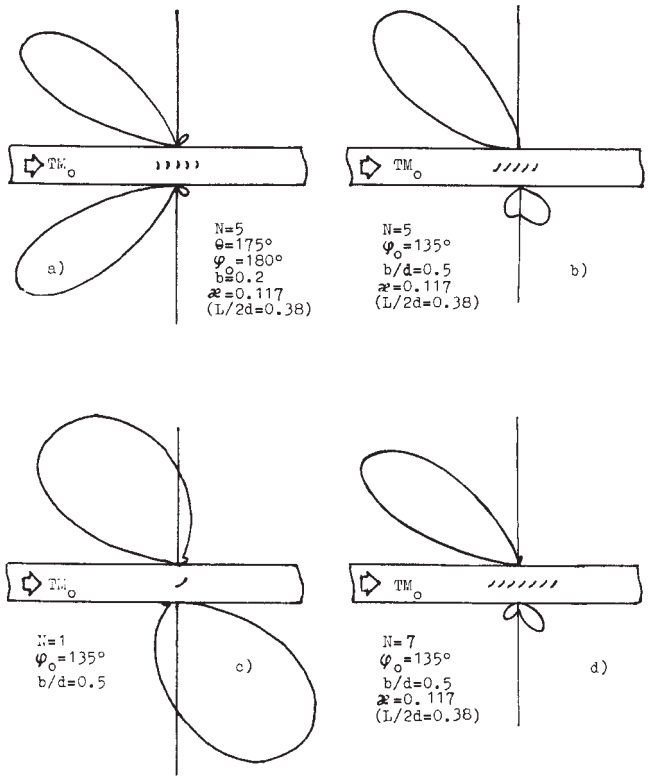

Figure 3 Normalized far-field scattering patterns for a grating of narrow strips

Figures 2(b), 2(c), and 2(d) correspond to the grating couplers of $N = 5$ wires of approximately the same radius but spaced at greater distances, so that $\kappa = 0.43$, 0.53, and 0.74, respectively. In general, the lobes of the scattering patterns are narrower as they are associated with forming the -1st Floquet space harmonic of similar infinite grating. Unlike the 0th harmonic which is locked inside the film, the -1st one is not subjected to the total internal reflection and radiates to the outer space after refracting at the interfaces. The larger the number of wires, the narrower the beams. If the period is increasing, the second (smaller) lobe of the pattern is observed detecting the launching of the -2nd harmonic, while the main lobe shifts toward endfire radiation.

Figure 3 demonstrates patterns due to the scattering from gratings of narrow circularly curved strips with parameters $\theta = 175°$ and $a/d = 0.33$. Although a single strip inhomogeneity radiates like a 2D dipole [Figure 3(c)], the grating of $N = 5$ elements can produce the scattering with a single main lobe provided that the strips are inclined [Figure 3(b)]. Otherwise the radiation is very much similar to that from a wire grating coupler [compare with Figure 2(a)]. By increasing the numberof strips one can enhance the directivity [see Figure 3(d)].

All the diffraction patterns presented in Figure 4 were computed for gratings of $N = 5$ screens with parameters $a/d = 0.35$, $b = 0$ and period $\kappa = 0.424$ ($L/2d = 1.35$). If the slits are narrow enough such screens display all the features of cavity-backed apertures. At $\theta = 30°$ [Figures 4(a), 4(b), and 4(c)] this corresponds to equiphase excitation of so-called Helmholtz resonant mode inside each of the slitted cylinders [6, 7]. This effect enhances significantly the amplitude of the radiated field. The slots here radiate as intensive secondary magnetic-line-current sources, and are excited practically independently on the exact positions of the slots.

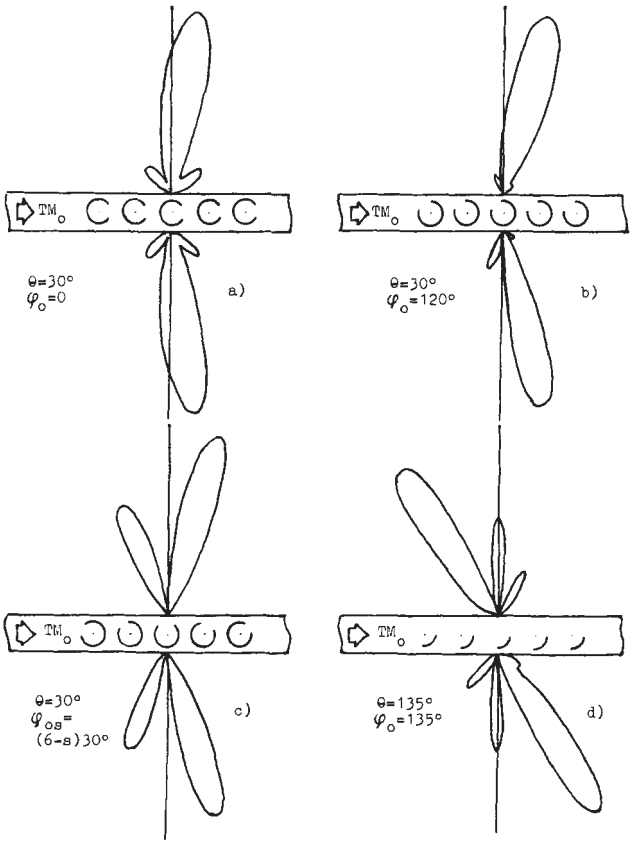

Figure 4 Normalized far-field scattering patterns for a grating of slitted circular cylinders

Indeed, if all the slots are at the same position as in Figures 4(a) and 4(b), there is a very small difference in far-field patterns. Even when the slots are positioned in an unidentical manner, as in Figure 4(c), the main features of the resonant scattering are maintained. By varying the angular widths of the screens one can change the pattern, as is demonstrated in Figure 4(d) for a grating of quartercircular strips.

So, we can conclude that although a grating coupler of circular wires is able to produce rather narrow beams of the scattered field, it cannot concentrate the radiation in a single direction. Unlike this one, a coupler of narrow strips can produce single-beam patterns, while a grating of cavity-baked slits can enhance the effectiveness of radiation.

REFERENCES

1. T. Tamir (Ed.), *Integrated Optics*, Springer, New York, 1979.
2. K. Ogawa, W. S. Chang, B. L. Sopori, and F. J. Rosenbaum, "Theoretical Analysis of Etched Grating Coupler for Integrated Optics," *IEEE J. Quantum Electron.*, Vol. QE-9, 1973, pp. 29–42.
3. C. C. Ghizoni, B. U. Chen, and C. L. Tang, "Theory and Experiments on Grating Coupler for Thin-Film Waveguides," *IEEE J. Quantum Electron.*, Vol. QE-12, 1976, pp. 69–73.
4. W. S. Park and S. R. Seshadri, "Theory of the Grating Coupler for a Ground-Dielectric-Slab Waveguide," *IEE Proc.*, Vol. H-132, June 1985, pp. 149–156.
5. M. Tomita, "Thin-Film Waveguide with a Periodic Groove Structure of Finite Extent," *JOSA*, Vol. A-6, Sept. 1989, pp. 1455–1464.
6. A. S. Andrenko and A. I. Nosich, "Resonant Scattering by Screen Inhomogeneities in Dielectric Slab Waveguide," *Proc. 3rd Asia-Pacific Microwave Conf.*, Tokyo, 1990, pp. 1175–1178.
7. A. I. Nosich and A. S. Andrenko, "Scattering and Mode Conversion by a Screen Inhomogeneity inside a Dielectric Slab Waveguide," *IEEE Trans. Microwave Theory Tech.*, Vol. MTT (to be published).

Received 12-9-91

Microwave and Optical Technology Letters, 5/7, 333–337

CCC 0895-2477/92/$4.00

AN UNIFIED THEORY OF ELECTROMAGNETIC MISSILES GENERATED BY AN ARBITRARY PLANE CURRENT SOURCE

Wen Geyi, Ruan Chengli, and Lin Weigan
Institue of Applied Physics
University of Electronic Science and Technology of China
Chengdu 610054, Peoples Republic of China

KEY TERMS

Electromagnetic missiles, plane current distribution, slow decrease of electromagnetic energy

ABSTRACT

In this article a generalized study of electromagnetic (EM) missiles has been presented. An EM missile source condition has been derived from an arbitrary plane current distribution, and our analysis shows that an arbitrary plane current distribution of finite size has the ability to launch an EM missile, i.e., to realize slow decrease of energy, on any axis perpendicular to the source plane so long as the axis has an intersection point with the source region. This important result reveals that the EM missiles are very much like light beams which do not diverge. © 1992 John Wiley & Sons, Inc.

1. INTRODUCTION

Electromagnetic (EM) missiles have been an interesting topic for several years and many practical EM missle sources have been investigated both analytically and experimentally. It was first realized by Wu that, under transient excitation, the energy transmitted by a current distribution in a plane to a far-away receiver can decrease much more slowly than the usual inverse square law r^{-2}. Such pulses are called electromagnetic missiles [1].

As far as the authors can determine, the discussion about electromagnetic missiles has so far been limited to the cases where the current sources are distributed either in a circular disk or a rectangle. What one can obtain from the present theories for a circular or a rectangular aperture is that the EM missle can exist on or very close to the center axis of the aperture, i.e., the axis of maximum radiation.

In this article we have presented a unified approach to the electromagnetic missiles generated by an arbitrary plane current distribution, based on the assumption that the transmitting current is a separable function of space and time, and a general EM missile source condition has been derived. Our analysis shows that an arbitrary plane current distribution is capable of launching an EM missile, i.e., to realize slow decrease of energy. Such an EM missile can exist not only on the center axis but also on any axis perpendicular to the source plane so long as the axis has an intersection point with the source region. This important result reveals that the EM missiles are very much like the light beams which do not diverge.